

NUMERICAL INVESTIGATION ON DYNAMIC CHARACTERISTICS OF HYDRODYNAMIC BEARING

by

Liangliang LI, Yunzhu LI, and Yonghui XIE*

Shaanxi Engineering Laboratory of Turbomachinery and Power Equipment,
School of Energy and Power Engineering, Xi'an Jiaotong University, Xi'an, China

Original scientific paper
<https://doi.org/10.2298/TSCI17S1201L>

In this paper, both the steady-state and transient-state of the films flow are investigated by CFD. The journal bearing dynamic characteristics such as the load capacity, damping and stiffness coefficients for several eccentricity, and length over diameter ratio (L/D) are obtained and compared with each other in different working conditions. Furthermore, the variation of various research parameters with eccentricity and L/D are also illustrated in detail.

Key words: hydrodynamic bearing, load capacity, eccentricity, L/D ratios, damping coefficient, stiffness coefficient

Introduction

Hydrodynamic bearing is one of the most widely used types of the sliding bearings in engineering applications. As for now, the research methods of hydrodynamic bearing mainly involve experimental investigation and numerical simulation. With the popularity of computer technology and the rapid development of CFD methods, CFD simulation has gradually become the mainstream method to obtain the dynamic characteristics of hydrodynamic bearing [1, 2].

Four stiffness coefficients and four damping coefficients were used to establish a flexible bearing-rotor system model by Lund [3], which revealed the eddy characteristic of the bearing-rotor system. And infinitesimal perturbation method was employed by Lund [4, 5] to obtain the linear stiffness and damping coefficients about journal equilibrium position. The numerical solution of the Reynolds equation was gained by Sivak and Sivak [6] using the improved Ritz method. The variation of stiffness and damping coefficients with large dynamic load of rotary compressor was studied by Hattori [7]. Dynamic coefficients under different perturbation amplitude were calculated by Qiu and Tieu [8], and the results emerged that the perturbation displacement and velocity should be less than 5% and 4%, respectively, to ensure the accuracy of damping and stiffness coefficient calculations. The non-linear properties of dynamic bearing under different L/D ratios are investigated by Sawicki and Rao [9], and the change rules of higher order damping and stiffness coefficients were described. The dynamic characteristics of hydrodynamic bearing lubricated with both Newtonian fluid and non-Newtonian fluid were studied by Gertzog *et al.* [10] using dynamic mesh technology, and the variation law of dimensionless friction with eccentricity was presented. The fluid film film was simulated using CFX-TASC flow and the damping and stiffness properties of the bearing were gained by

* Corresponding author, e-mail: yhxie@mail.xjtu.edu.cn

Guo *et al.* [11] using different methods, which verified the calculation accuracy of the damping and stiffness coefficients by numerical method. Experimental method was adopted by Lijesh *et al.* [12] to investigate the damping and stiffness properties of non-contact passive magnetic bearings, and a hybrid bearing was proposed through pendulum test. The non-linear characteristics of oil film were obtained under the large amplitude movement of journal by Wood *et al.* [13], considering the higher order terms in the bearing reaction expansion. The minimum square method was adopted by Muller-Karger *et al.* [14] to adjust dynamic coefficients, and the calculation results revealed that the non-linearity depends on the size and shape of the orbital motion. The aim of the paper is to investigate both the steady- and transient-states of the films flow with the help of CFD.

The CFD theory and dynamic characteristics calculation method

At present, commercial software has been widely used in the calculation of sliding bearings [15, 16]. Solving the Reynolds equation is an important issue in the numerical solution of hydrodynamic bearings [17, 18]. The dynamic Reynolds equation is usually used as a lubrication equation for calculating the stiffness and damping coefficients of hydrodynamic bearings [19]. The Reynolds equation describing the motion of the fluid film is:

$$\nabla \left(\frac{h^3}{12\mu} \nabla p \right) = \nabla(h\bar{U}) - V \quad (1)$$

where \bar{U} is the velocity of journal surface, and V is the film velocity.

Generally, the oil film can only withstand positive pressure. When the film pressure drops down to the atmosphere pressure, rupture of film or cavitation occurs. The half-Sommerfeld boundary condition, which divides the whole oil film into complete oil film zone and rupture zone, specifies the magnitude of static pressure in rupture zone as zero Pascal.

The damping and stiffness coefficients can be obtained by finite difference method in the case of small disturbance. According to perturbation theory, oil film force could be linearized. The increment of fluid film force components can be expressed:

$$\begin{pmatrix} \Delta F_x \\ \Delta F_y \end{pmatrix} = \begin{pmatrix} K_{xx} & K_{xy} \\ K_{yx} & K_{yy} \end{pmatrix} \begin{pmatrix} \Delta x \\ \Delta y \end{pmatrix} + \begin{pmatrix} C_{xx} & C_{xy} \\ C_{yx} & C_{yy} \end{pmatrix} \begin{pmatrix} x' \\ y' \end{pmatrix} \quad (2)$$

where ΔF_x and ΔF_y are the change of oil film force in two directions, respectively, K_{xx} and K_{yy} are direct stiffness coefficients, K_{xy} and K_{yx} are cross stiffness coefficients, C_{xx} and C_{yy} are direct damping coefficients, C_{xy} and C_{yx} are cross damping coefficients, Δx and Δy are perturbation displacement in two directions, and x' and y' are perturbation velocity in two directions.

The stiffness and damping coefficients can be calculated by eq. (3):

$$\begin{aligned} K_{xx} &= \frac{\Delta F_{dxx}}{\Delta x} & K_{yx} &= \frac{\Delta F_{dyx}}{\Delta x} & C_{xx} &= \frac{\Delta F_{vxx}}{x'} & C_{yx} &= \frac{\Delta F_{vyx}}{x'} \\ K_{xy} &= \frac{\Delta F_{dxy}}{\Delta y} & K_{yy} &= \frac{\Delta F_{dyy}}{\Delta y} & C_{xy} &= \frac{\Delta F_{vxy}}{y'} & C_{yy} &= \frac{\Delta F_{vyy}}{y'} \end{aligned} \quad (3)$$

where ΔF_{dij} is the change of oil film force caused by perturbation displacement, and ΔF_{vij} is the change of oil film force caused by perturbation velocity.

Variation of bearing performance under different eccentricity

Consider a typical cylindrical journal bearing. Assume the diameter of the bearing $D = 60$ mm with the length $L = 60$ mm and radial clearance $h_0 = 30$ μm . In the calculation, lubricant grade is HU-20, the density of lubricating oil is 960 kg/m^3 , average dynamic viscosity coefficient is $\mu = 0.0125$ $\text{Pa}\cdot\text{s}$ and the influence of temperature on viscosity is ignored. Laminar flow model and SIMPLEC pressure-velocity coupling algorithm are adopted in the calculation. The operating pressure is set to 101325 Pa. To simplify the geometry, one side of the oil film clearance is used as an inlet and the other as an outlet. The boundary conditions are *pressure inlet* and *pressure outlet*, respectively, with gauge pressure at zero Pa. The outer surface of oil film is modeled as *stationary wall*, while the inner surface is modeled as *moving wall*, with an absolutely rotational speed of 500 rad/s. The position of rotation axis is determined by the eccentricity, ε .

In the actual operating condition, there exists cavitation in the non-loaded region. Therefore, half-Sommerfeld boundary condition is adopted to ensure that the numerical results are in consistent with the actual operating condition. The FLUENT DEFINE_ON_DEMAND macro is employed for the definition of half-Sommerfeld condition, which sets the value of negative gauge pressure to the value of operating pressure.

In the common operating eccentricity range of hydrodynamic bearing, the pressure distribution and load capacity of oil film can be obtained under half-Sommerfeld boundary condition by CFD simulation. Figure 1 shows the load capacity and the attitude angle for several eccentricity in the range of $[0.2, 0.7]$. With the increase of eccentricity, the hydrodynamic effect in wedge becomes more and more obvious and the maximum bearing capacity shows a tendency of accelerated increase. It is observed that the attitude angle approximately approaches 90° when the eccentricity is closed to zero. And the attitude angle decreases rapidly with the eccentricity. Results extracted in fig. 1 illustrate that the convergent wedge decreases gradually and moves toward the minimum film thickness direction, and the load center moves in the same direction, resulting in a gradual decline of the attitude angle.

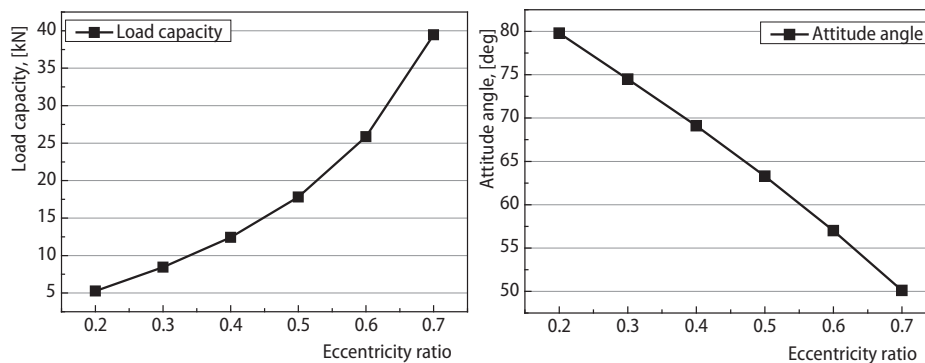


Figure 1. The influence of eccentricity on load capacity and attitude angle

Figure 2 shows the pressure distribution of the given model for relative eccentricities $\varepsilon = 0.3, 0.5$, and 0.7 . It is observed that the area of convergent wedge decreases with the eccentricity, and the hydrodynamic effect region moves towards the minimum film thickness ($\theta = \pi$) direction. Results from fig. 2 indicate that the effective bearing area reduces gradually and the local stress rises dramatically under heavy load. Figure 3 shows the pressure distribu-

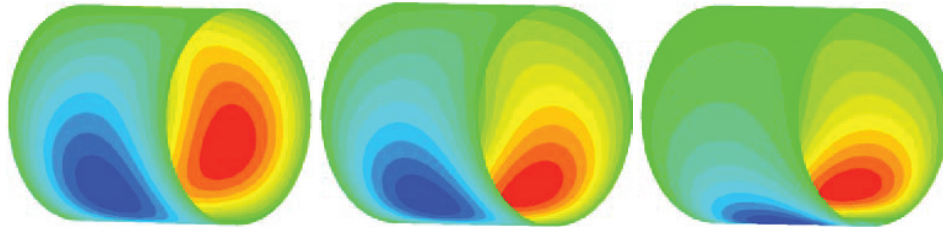


Figure 2. Pressure distribution for different eccentricity (followed by $\varepsilon = 0.3, \varepsilon = 0.5, \varepsilon = 0.7$)
(for color image see journal web site)

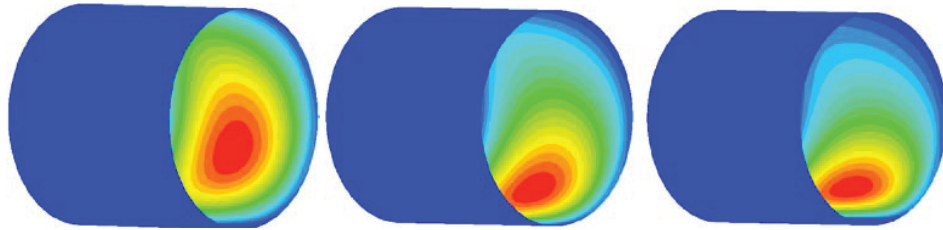


Figure 3. Pressure distribution in half-Sommerfeld boundary condition
(followed by $\varepsilon = 0.3, \varepsilon = 0.5, \varepsilon = 0.7$) (for color image see journal web site)

tion in half-Sommerfeld boundary condition, and the results are consistent with the positive pressure area in fig 2.

Dynamic mesh technology is adopted to obtain the dynamic coefficients of bearings. Figure 4 shows the stiffness coefficient including direct stiffness and cross stiffness *vs.* the eccentricity of the bearing with the L/D ratio specified as 1. The direct stiffness coefficient increases rapidly with the eccentricity, and the increase rate of stiffness coefficient in loaded direction, K_{yy} , is greater than that in the non-loaded direction, K_{xx} . The cross stiffness coefficient, K_{xy} , changes slightly with the eccentricity, which indicates the perturbation in the loaded direction and the change of the eccentricity have little effect on the non-loaded direction. In contrast, the value of K_{yx} decreases rapidly, which indicates that the perturbation in non-loaded direction has great impact on the loaded direction.

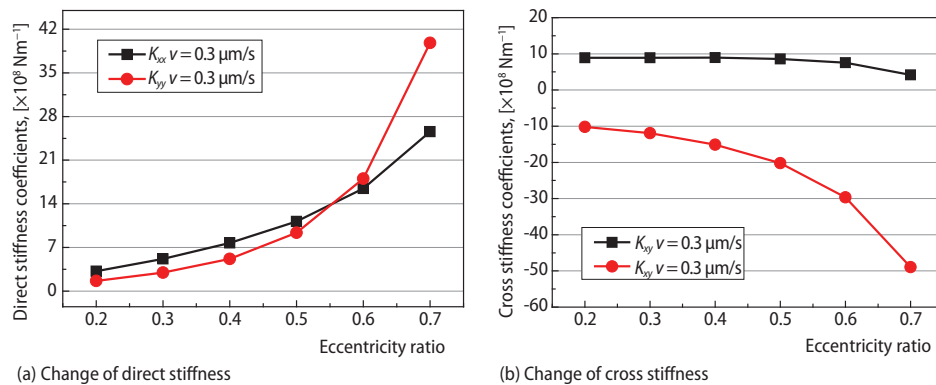


Figure 4. The variation law of stiffness coefficient with eccentricity

Figure 5 shows the relation between the damping coefficient and the eccentricity of the bearing. Similar to the change rules of stiffness coefficient, the direct damping coefficient increases with the eccentricity, and the increase rate of damping coefficient in loaded direction, C_{yy} , is greater than that in the non-loaded direction, C_{xx} . Both the cross-damping coefficients, C_{xy} and C_{yx} , show a tendency of decrease, and the changing speed of C_{xy} and C_{yx} is approximately the same, which declares that the perturbation velocity influences the cross-direction oil film force in a quite equal degree.

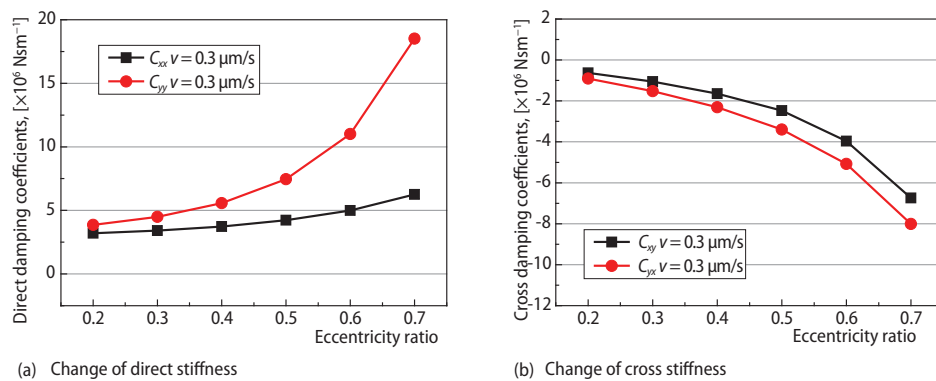


Figure 5. The variation law of damping coefficient with eccentricity

Variation of bearing performance for different L/D ratios

Steady analysis of the hydrodynamic bearing with $\varepsilon = 0.5$ is carried out for different L/D ratios, $L/D = 0.6$, $L/D = 0.8$, $L/D = 1.0$, $L/D = 1.2$, and $L/D = 1.4$, respectively. Figure 6 shows the load capacity and attitude angle of oil film obtained in half-Sommerfeld boundary condition. Because the area of the convergent wedge is approximately proportional to L/D ratio, the load capacity of the bearing increases as the L/D ratios increasing. Additionally, the attitude angle also increases with L/D ratio in fig. 6. As previously analyzed, the area of loaded region is slightly extended along the circumference with L/D ratio, and the center of the loaded region moves towards the vicinity of $\theta = 0$, which causes a slightly increase of attitude angle.

Figure 7 shows the pressure distribution of the given model for different L/D ratios ($\varepsilon = 0.3$, $\varepsilon = 0.5$, $\varepsilon = 0.7$). The area of the loaded region along the axial direction is obviously

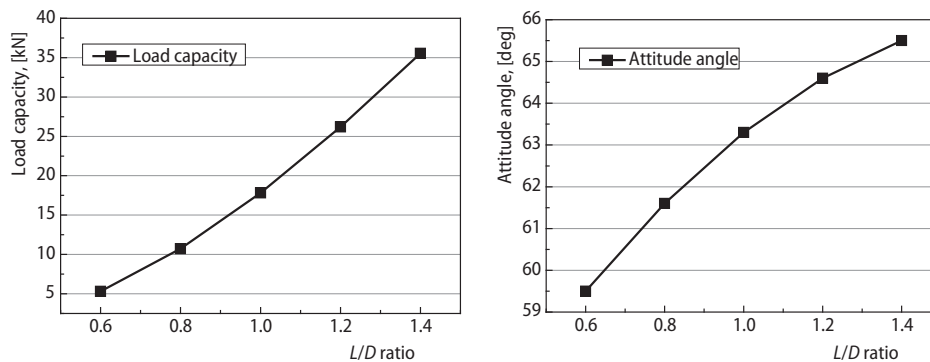


Figure 6. The influence of L/D ratios on load capacity and attitude angle

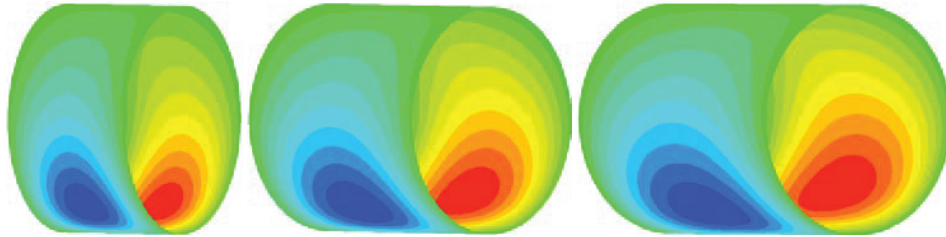


Figure 7. Pressure distribution for different L/D ratios (followed by $L/D = 0.6$, $L/D = 1$, $L/D = 1.4$)
(for color image see journal web site)

expanded with L/D ratios, while it is slightly expanded along the circumferential direction. The previous results indicate that the loaded capacity of the bearing increases with the L/D ratio. Figure 8 shows the true pressure distribution of the oil film under the half-Sommerfeld boundary, and the distribution of the loaded area is consistent with the positive pressure zone in fig. 7.

Figure 9 shows the variation of the stiffness coefficient with L/D ratio. It can be seen that the direct stiffness coefficients increase with the increase of L/D ratio, in addition, the increase rate of stiffness coefficient in non-loaded direction, K_{xx} , is greater than that in the loaded direction, K_{yy} . It is obvious that the increase of L/D ratio enhance the stability of hydrodynamic journal bearing. As for the cross stiffness, their absolute value increase with the L/D ratio, and the absolute change rate of cross stiffness coefficient in non-loaded direction, K_{xy} , is smaller than that in the loaded direction, K_{yx} . The change law indicates that the perturbation displacement in the perturbation in non-loaded direction has a relatively greater influence on the loaded direction than that on the contrary.

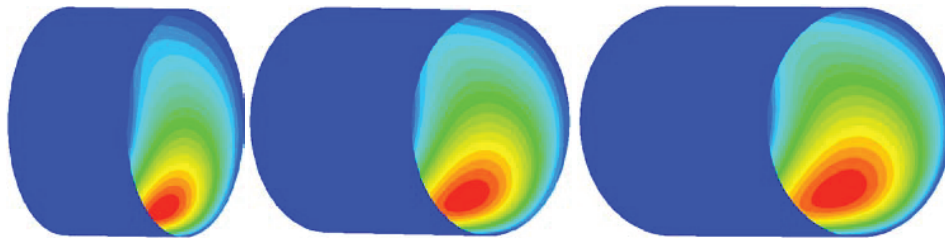


Figure 8. Pressure distribution under half-Sommerfeld boundary condition
(followed by $L/D = 0.6$, $L/D = 1$, $L/D = 1.4$) (for color image see journal web site)

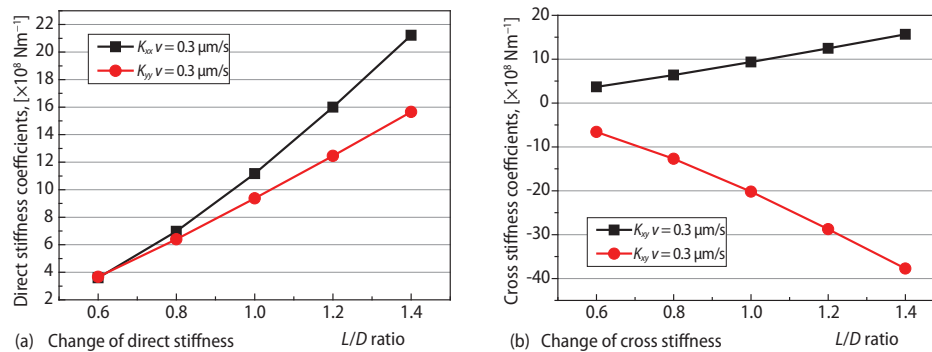


Figure 9. The variation law of stiffness coefficient with L/D ratio

Figure 10 shows the variation of the damping coefficient with L/D ratio. It can be seen that the direct damping coefficient increases with the increase of L/D ratio, and the damping coefficient in the loaded direction is larger than that in the non-load direction. The cross-damping coefficient decreases with the increase of L/D ratio, and the perturbation velocity in the non-loaded direction has a relatively greater influence on the loaded direction.

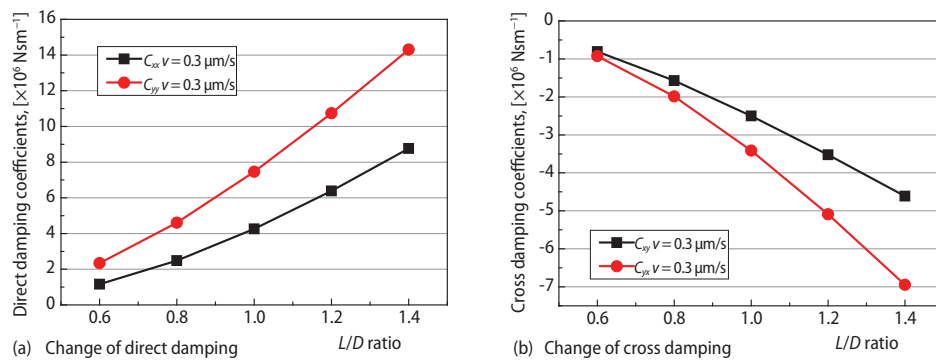


Figure 10. The variation law of damping coefficient with L/D ratio

Conclusion

In this work, we presented the steady- and transient-states of the films flow are investigated with the aid of CFD. The load capacity, damping and stiffness coefficients for several eccentricity and length over diameter ratio were discussed in details. The load capacity of the bearing shows a tendency of increase with the increase of the eccentricity and the L/D ratio. Moreover, the direct stiffness in non-loaded direction increases faster than that in loaded direction, while the direct damping of the load direction increases faster than that in non-loaded direction.

Nomenclature

C – damping coefficient, [Nsm^{-1}]
 D – diameter of bearing, [m]
 e – eccentricity, [m]
 F – oil film force, [N]
 h – film thickness, [m]
 h_0 – clearance, [m]
 K – stiffness coefficient, [Nm^{-1}]
 L – bearing length, [m]
 p – pressure, [Pa]

U – journal velocity, [ms^{-1}]
 V – film velocity, [ms^{-1}]

Greek symbols

ε – relative eccentricity ($= e/h_0$), [–]
 θ – bearing angle, [$^\circ$]
 μ – viscosity, [$\text{Pa}\cdot\text{s}$]
 φ – attitude angle, [$^\circ$]
 Ω – rotational speed of journal, [rad s^{-1}]

References

- [1] Kirk, R. G., et al., PC-Based Analysis of Turbomachinery Vibration, *Shock and Vibration Digest*, 31 (1999), 6, pp. 449-454
- [2] Guo, Z., Kirk, R. G., Analysis of Externally Pressurized Fluid-Film Bearings for High-Speed Rotating Machinery, *Proceedings, ISCORMA*, Lake Tahoe, Cal., USA, 2001, Vol. 1, pp. 20-24
- [3] Lund, J. W., The Stability of an Elastic Rotor in Journal Bearings with Flexible, Damped Supports, *Journal of Applied Mechanics*, 4 (1965), 32, pp. 911-920
- [4] Lund, J. W., Thomsen, K. K., A Calculation Method and Data for the Dynamic Coefficients of Oil-Lubricated Journal Bearings, *Topics in Fluid Film Bearing and Rotor Bearing System Design and Optimization*, ASME, New York, USA, 1978, pp. 1-28

- [5] Lund, J. W., Review of the Concept of Dynamic Coefficients for Fluid Film Journal Bearings, *ASME J. Tribol.*, 109 (1987), 1, pp. 37-41
- [6] Sivak, B., Sivak, M., The Numerical Solution of the Reynolds Equation by a Modified Ritz Method, *Wear*, 72 (1981), 3, pp. 371-376
- [7] Hattori, H., Dynamic Analysis of a Rotor-Journal Bearing System with Large Dynamic Loads: Stiffness and Damping Coefficient Variations in Bearing Oil Films, *Jsm International Journal*, 36 (2008), 2, pp. 251-257
- [8] Qiu, Z. L., Tieu, A. K., The Effect of Perturbation Amplitudes on Eight Force Coefficients of Journal Bearings, *Tribology Transactions*, 39 (1996), 2, pp. 469-475
- [9] Sawicki, J. T., Rao, T. A., Nonlinear Model for Prediction of Dynamic Coefficients in a Hydrodynamic Journal Bearing, *International Journal of Rotating Machinery*, 10 (2004), 6, pp. 507-513
- [10] Gertzog, K. P., *et al.*, CFD Analysis of Journal Bearing Hydrodynamic Lubrication by Bingham Lubricant, *Tribology International*, 41 (2008), 12, pp. 1190-1204
- [11] Guo, Z., *et al.*, Application of CFD Analysis for Rotating Machinery: Part 1—Hydrodynamic, Hydrostatic Bearings and Squeeze Film Damper, *Proceedings*, ASME Turbo Expo 2003, Collocated with the 2003 International Joint Power Generation Conference. American Society of Mechanical Engineers, Atlanta, Geo., USA, pp. 651-659, 2003
- [12] Lijesh, K.P., *et al.*, Stiffness and Damping Coefficients for Rubber Mounted Hybrid Bearing, *Lubrication Science*, 26 (2014), 5, pp. 301-314
- [13] Wood, K. L., *et al.*, A Nonlinear Dynamic Model with Confidence Bounds for Hydrodynamic Bearings, *Journal of Tribology*, 120 (1998), 3, pp. 595-604
- [14] Muller-Karger, C. M., *et al.*, Derivation of Hydrodynamic Bearing Coefficients Using the Minimum Square Method, *Journal of Tribology*, 119 (1997), 4, pp. 802-807
- [15] Makino, T., Mori, I. I., Entry Flow and Pressure Jump in Submerged Multi-Pad Bearings and Grooved Bearings, *Journal of Tribology*, 114 (1992), 2, pp. 370-378
- [16] Keogh, P. S., On the Dynamic Thermal State in a Hydrodynamic Bearing with a Whirling Journal Using CFD Techniques, *Journal of Tribology*, 118 (1996), 2, pp. 356-363
- [17] Pinkus, O., *et al.*, *Theory of Hydrodynamic Lubrication*, McGraw-Hill, New York, USA, 1961
- [18] Nicholas, J. C., *et al.*, Stiffness and Damping Coefficients for the Five-Pad Tilting-Pad Bearing, *ASLE Transactions*, 22 (1979), 2, pp. 113-124
- [19] Ghosh, M. K., *et al.*, Steady-State and Dynamic Behaviour of Multi-Recess Hybrid Oil Journal Bearings, *Journal of Mechanical Engineering Science*, 21 (1979), 5, pp. 345-351